Relationship between structural and dynamic properties of Al-rich Al-Cu melts: Beyond the Stokes-Einstein relation

N. Jakse and A. Pasturel

Sciences et Ingénierie des Matériaux et Procédés (SIMAP), UMR CNRS 5266, Grenoble Université Alpes, BP 75, 38402 Saint-Martin d'Hères Cedex, France

(Received 19 July 2016; revised manuscript received 28 September 2016; published 12 December 2016)

We perform *ab initio* molecular dynamics simulations to study structural and transport properties in liquid $Al_{1-x}Cu_x$ alloys, with copper composition $x \leqslant 0.4$, in relation to the applicability of the Stokes-Einstein (SE) equation in these melts. To begin, we find that self-diffusion coefficients and viscosity are composition dependent, while their temperature dependence follows an Arrhenius-type behavior, except for $x = 0.4$ at low temperature. Then, we find that the applicability of the SE equation is also composition dependent, and its breakdown in the liquid regime above the liquidus temperature can be related to different local ordering around each species. In this case, we emphasize the difficulty of extracting effective atomic radii from interatomic distances found in liquid phases, but we see a clear correlation between transport properties and local ordering described through the structural entropy approximated by the two-body contribution. We use these findings to reformulate the SE equation within the framework of Rosenfeld's scaling law in terms of partial structural entropies, and we demonstrate that the breakdown of the SE relation can be related to their temperature dependence. Finally, we also use this framework to derive a simple relation between the ratio of the self-diffusivities of the components and the ratio of their partial structural entropies.

DOI: 10.1103/PhysRevB.94.224201

I. INTRODUCTION

Liquid phase dynamics plays a critical role in phase transformations like crystal or glass formation, and controlling such transformation pathways requires a comprehensive study of diffusivity and viscosity as a function of temperature. In particular, structural and transport properties of melts and their interplay represent an important issue in condensed matter physics and material science, not only regarding fundamental aspects, but also for applications. They have a strong impact on numerous academic studies on solidification, for instance in dendritic growth, and they also play important roles in the processing of commercial lightweight alloys, such as aluminum-based alloys, for many applications in the automotive and aeronautic industry. Therefore, the knowledge of such properties prior to solidification is of high interest in designing new workable alloys, and within this strategy, the influence of the structural characteristics of the liquid phase on transport properties that can be tuned by additional alloying elements plays a prominent role.

The study of transport properties of liquids has been often based on the Stokes-Einstein (SE) relation, which predicts that the self-diffusion coefficient D is proportional to (T/η), where η is the viscosity and T is the temperature. More specifically, the SE relation can be written as $D\eta/k_BT = 1/C\pi R_{SE}$, where R_{SE} is an effective radius of particles immersed in a viscous fluid medium. The dimensionless constant C is taken as 6 in the original SE relation, while a value of 4, as used in the present paper, is also reported, depending on the hydrodynamic boundary conditions assumed. Quite remarkably, the SE relation was found to work well for many monatomic liquids [1] and molecular liquids [2], and its applicability in liquid alloys is well accepted in common literature [3], although it is not clear at all why this should be the case.

In fact, the breakdown of the SE relation in the deep undercooling regime is even considered one of the hallmarks of transport properties characterized by a strong decoupling of diffusion from viscosity [4–6]. This decoupling is a significant indication that different ways to measure relaxation times lead to different answers and thus is a strong hint of the existence of broad "distributions" of relaxation time scales [7]. This leads to the existence of spatially heterogeneous dynamics or dynamic heterogeneities (DHs) [3,7–10], an Arrhenius to non-Arrhenius crossover of dynamics [3], or a change in the diffusion mechanisms, such as jump diffusion [11] or the self-hole filling mechanism [12]. The breakdown of the SE relation might also give rise to a crossover toward a fractional SE relation [13] that was associated with the development of a medium-range order [14] or a change in the friction coefficient for diffusion [15].

In the high-temperature liquid regime, the situation is more controversial since the SE relation is taken for granted in many experimental studies, although there is also evidence of its breakdown [16]. More particularly, Brillo *et al.* [17] have shown that the SE relation is valid in liquid $Al_{80}Cu_{20}$ above 1400 K, which is 400 K higher than its liquidus temperature. Below 1400 K, the SE relation fails, giving rise to an effective SE radius of the copper species that increases with decreasing temperature and becomes greater than the known covalent radius of copper atoms. A breakdown of the SE relation also has been observed experimentally in Ni-Zr alloys [18] characterized in that case by values of $D_{Ni}\eta$ that are constant with temperature. It has been pointed out that a match of experimental values of diffusion and viscosity with the SE relation in the vicinity of the melting temperature would lead to an unrealistic SE radius for Ni. Using computer simulations, we have recently shown that the SE relation fails for liquid $Al_{80}Ni_{20}$ and $Al_{80}Cu_{20}$ alloys, while it is valid for $Al_{80}Zn_{20}$ alloys [3]. Han *et al.* [12] have also evidenced the high-temperature breakdown of the SE relation in liquid Cu_8Zr_3.

Can the breakdown of the SE relation in the liquid regime be considered like an intrinsic property of a melt, or does it occur only in some alloying compositions in relation to local ordering

effects? Are there other reasons, like the existence of dynamic heterogeneities in the liquid phase? Intrinsic properties of chemical species present in an alloy will impose specificity of the chemical and topological short-range order. For instance, we have shown that the degree of icosahedral short-range order (ISRO) in a pure metallic liquid depends on the nature of the metal [19]. Moreover, in liquid metallic alloys like Al-based alloys, we have demonstrated that alloying effects lead to a local chemical short-range order (CSRO) that may enhance or disfavor ISRO [20]. This interplay between CSRO and ISRO will influence transport properties as a function of composition and temperature and eventually may cause a chemically induced heterogeneity far above the liquidus temperature, as was recently observed in a glass-forming melt [21].

To elucidate these questions, we propose to use *ab initio* molecular dynamics (AIMD) simulations to study the composition and temperature dependence of structural and dynamic properties of liquid $Al_{1-x}Cu_x$ alloys, $x \leqslant 0.4$, as well as their relationship through the SE relation. The choice of the Al-Cu alloys on the Al-rich side is guided by the occurrence of an appreciable degree of CSRO in the liquid phase [22] and the existence of a broad temperature range of the liquid phase from pure Al up to 0.4, as observed in the experimental phase diagram. Moreover, experimental data for Cu diffusion coefficients are available, although relatively scarce [15,23,24], while a relatively large number of viscosity measurements have been reported by different investigators [25–31].

First, we find that self-diffusion coefficients and viscosity are composition dependent, while their temperature dependence follows an Arrhenius-type behavior, except for $x = 0.4$ below $T = 1200$ K. Then, from the study of the temperature dependence of the ratio $D\eta/(k_BT)$, we point out a few important observations: (i) We determine that the temperature dependence of $D_{Cu}\eta/(k_BT)$ depends on the Cu composition, this effect being much less pronounced for $D_{Al}\eta/(k_BT)$. (ii) We emphasize the difficulty of extracting effective atomic radii corresponding to interatomic distances found in liquid phases. (iii) We show a correlation between transport properties and local ordering around each species through the pair excess entropy, or the so-called structural entropy [32,33]. (iv) We use these findings to reformulate the SE equation within the framework of Rosenfeld's scaling law in terms of the partial structural entropies, and we demonstrate that the breakdown of the SE relation in the liquid regime can be related to their temperature dependence. (v) Finally, our approach allows the derivation of a simple relation between the ratio of the self-diffusivities of the components and the ratio of their partial-pair excess entropies.

II. COMPUTATIONAL METHODS

A. Molecular dynamics simulations

AIMD simulations of liquid $Al_{1-x}Cu_x$ alloys with $x = 0.1$, 0.2, 0.3, and 0.4 were carried out using the *ab initio* total energy and molecular dynamics of the Vienna *Ab initio* Simulation Package (VASP) [34]. All the dynamical simulations were performed in the local density approximation [35] and using projected augmented plane waves with a plane-wave cutoff of 270 eV. Newton's equations of motion were integrated using the Verlet algorithm in the velocity form with a time step of 1.5 fs within the constant number, volume, and temperature (NVT) ensemble by means of a Nosé thermostat to control temperature.

Some 256 atoms with the desirable composition are arranged in a cubic simulation box with standard periodic boundary conditions. Only the Γ point is used to sample the Brillouin zone. We have shown that such approximations reproduce the transport properties of liquid aluminum correctly [36].

The liquid samples were first prepared at a temperature well above the highest studied, namely 2500 K, for all compositions by performing a run of 30 ps to reach thermal equilibrium. This was followed by a cooling to the successively lower desired temperatures for the given alloy at a rate of 3×10^{12} K/s. For all Al-Cu alloys, we have considered five temperatures: 1000, 1200, 1400, 1600, and 1795 K. At each temperature, the volume V of the simulation cell was chosen to reproduce the experimental densities [37]. The pressures calculated in the simulation cells do not exceed 0.9 GPa, with a typical fluctuation of 1.2 GPa. Therefore, structural and dynamic properties are not influenced by pressure effects. After an equilibration of 30 ps at the studied temperature, the run was continued for 80 ps to produce the physical quantities described below. For pure liquid Al and Cu, we have used our results from Ref. [19], which we have extended here for Al in the temperature range between 1400 and 1700 K, using the same simulation procedure.

B. Self-diffusion and viscosity

In the present paper, we determine self-diffusion coefficients and viscosity of liquid $Al_{1-x}Cu_x$ alloys as follows: To begin, self-diffusion coefficients are related to the individual atom displacements through the mean square displacement (MSD) for each chemical species $i (i = \text{Al, Cu})$,

$$R_i^2(t) = \frac{1}{N_i}\sum_{k=1}^{N_i}\langle[\mathbf{r}_k(t+t_0) - \mathbf{r}_k(t_0)]^2\rangle_{t_0}. \quad (1)$$

In Eq. (1), $\mathbf{r}_k(t)$ is the position of atom k of species i at time t, and angle brackets represent the average over time origin t_0. The self-diffusion coefficient D_i is then computed from the long time slope of $R_i^2(t)$,

$$D_i = \lim_{t\to\infty}\frac{R_i^2(t)}{6t}. \quad (2)$$

D_i can be also calculated from the well-known Green-Kubo time integral of function $\Psi_i(t)$,

$$D_i = \frac{1}{3}\int_0^\infty \Psi_i(t)dt, \quad (3)$$

with

$$\Psi_i(t) = \frac{1}{N_i}\sum_{k=1}^{N_i}\langle\mathbf{v}_k(t+t_0)\times\mathbf{v}_k(t_0)\rangle_{t_0} \quad (4)$$

as the velocity autocorrelation function for species i obtained from the velocity $\mathbf{v}_k(t)$ of atom k of species i at time t. Comparison of the numerical values of the self-diffusion coefficients calculated from Eqs. (2) and (3) was done to check the consistency of the simulations.

The shear viscosity is computed by a direct method using the transverse current-current correlation function $C_T(q,t)$, as in our previous paper [36]. In brief, $C_T(q,t)$ is defined as

$$C_T(q,t) = \frac{1}{N}\langle J_T^*(q,t) J_T(q,t)\rangle, \tag{5}$$

where $J_T(q,t)$ is the transverse current, which can be determined along the x direction as

$$J_T(q,t) = \sum_{p=1}^{N} v_{p,x}(t)\exp[jqz_p(t)], \tag{6}$$

where the quantity $v_{p,x}(t)$ is the x component of the velocity of atom p. Two formally identical expressions can be written for y and z directions, from which the transverse current $J_T(q,t)$ can be evaluated independently, giving rise to the same result.

The zero-limit Laplace transform $\tilde{C}_T(q,w=0)$ gives rise to the q-dependent shear viscosity

$$\eta(q) = \frac{\rho k_B T}{mq^2 \tilde{C}_T(q,w=0)}, \tag{7}$$

where k_B and m correspond, respectively, to Boltzmann's constant and the weighted average atomic mass, and ρ is the number density. The shear viscosity η is thus obtained at the hydrodynamic limit of $\eta(q)$; namely, at $q=0$ the simulated value of $\eta(q)$ is extrapolated efficiently with the function designed initially to represent the viscosity of a dense hard-sphere system [38]

$$\eta(q) = \frac{\eta}{1+a^2q^2}. \tag{8}$$

We have shown in our preceding papers [36,39] that this procedure leads to reliable values of shear viscosity for metallic liquids with an uncertainty on the order of 0.2 mPa s.

C. Identification of local ordering

To identify local ordering of $Al_{1-x}Cu_x$ alloys, we first compute their partial-pair correlation functions $g_{ij}(r)(i,j = \text{Al, Cu})$ obtained from 1000 independent equilibrated configurations. We refer the reader to Refs. [1] and [40] for a detailed description of standard techniques to extract them. The partial nearest neighbor coordination numbers are then calculated by integrating the appropriate partial radial distribution functions $\text{RDF}_{ij}(r) = x_j 4\pi\rho r^2 g_{ij}(r)$ (ρ being the atomic density) up to the first minimum of the corresponding $g_{ij}(r)$. Note that we have also used these coordination numbers to discuss the CSRO through the Warren parameter [20].

To go beyond the angular averaged properties obtained from pair correlation functions and the coordination numbers, several methods have been proposed. Among them, the common neighbor analysis (CNA) [41] in which the local symmetry is determined on smaller basic units, namely atomic pairs, allowing us to discriminate between various local topologies, like face-centered-cubic (fcc), hexagonal close-packed (hcp), body-centered-cubic (bcc), and icosahedral, as well as more complex polytetrahedral environments. We have already used this approach to study local structural ordering in liquid Al-Ni alloys [42,43] and to reveal the high degree of icosahedral ordering. Results obtained in this paper are based on the same approach, and we refer the reader to Ref. [44] for a detailed description of the method.

III. RESULTS AND DISCUSSION

A. Dynamic properties of $Al_{1-x}Cu_x$ alloys

In a first step, we consider the temperature and composition dependence of self-diffusion coefficients, D_{Al} and D_{Cu}. They have been calculated either from MSD curves using Eq. (2) or from the velocity autocorrelation functions using Eq. (3). For all compositions and temperatures, both methods give a result within an error bar of 0.03 $Å^2$/ps, indicating that simulations are well equilibrated. We report in Fig. 1(a) their evolution with temperature for each composition, and we have also included results for pure Al and Cu liquids. We observe that D_{Cu} in alloys is higher than that of pure liquid Cu, the difference being

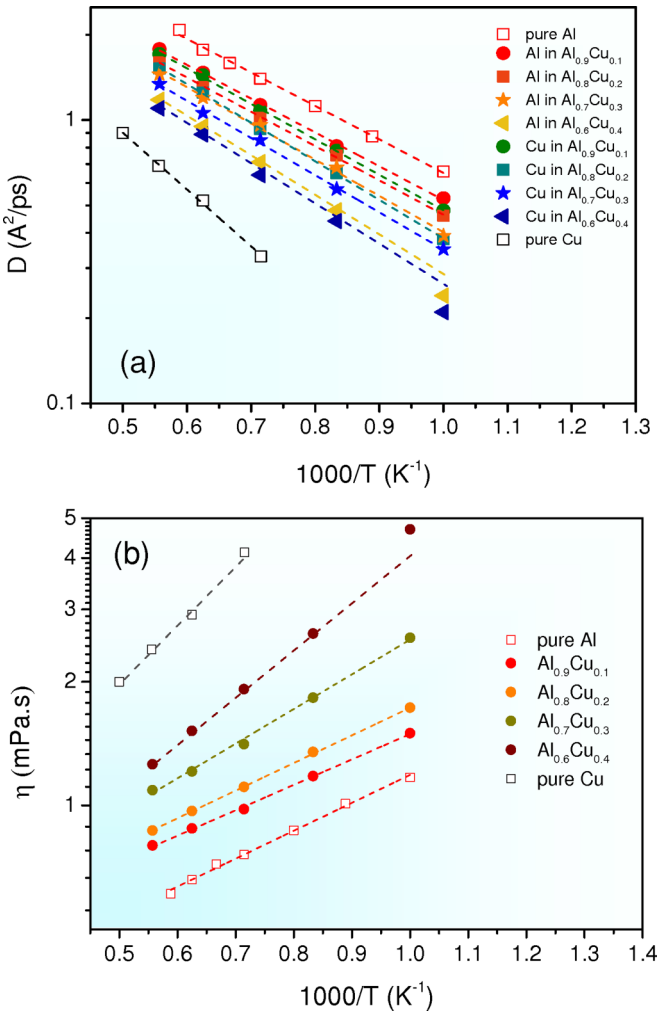

FIG. 1. (a) Calculated self-diffusion coefficients as a function of inverse temperature for Al-Cu alloys from *ab initio* molecular dynamics simulations for all compositions. Calculated values for pure elements are also included. Dashed lines are Arrhenius fits to AIMD results for alloys, as well as for pure elements Al and Cu are included in the corresponding panels. For $x = 0.4$ the Arrhenius fits are performed on the highest temperature. (b) Calculated viscosities as a function of inverse temperature for Al-Cu alloys, as well as for those of the pure elements.

TABLE I. Activation energies for self-diffusion (E_D) and viscosity (E_η) obtained from an Arrhenius fit of AIMD simulations as a function of Cu composition and compared with values found in the literature.

Al-Cu	E_D(kJ/mol)Al	E_D(kJ/mol)Cu	E_η(kJ/mol)	E_D^{Lit}(kJ/mol)Al	E_D^{Lit}(kJ/mol)Cu	E_η^{Lit}(kJ/mol)
Al	− 24.1 [19]		11.1 [19]	− 26.4 [67,68]		10.9 [31]
$Al_{90}Cu_{10}$	− 24.8	− 25.4	11.9		− 19.0 [23,24]	15.3 [29]
						12.8 [30]
						16.0 [31]
$Al_{80}Cu_{20}$	− 25.2	− 25.8	12.8	− 25.2 [45]	− 28.7 [50]	13.1 [30]
					− 32.8 [17]	13.2 [31]
					− 21.0 [23,24]	
$Al_{80}Cu_{30}$	− 25.5	− 25.8	16.7			16.1 [30]
						23.6 [31]
$Al_{60}Cu_{40}$	− 30.5	− 30.7	22.8	− 20.6 [45]	− 19.7 [45]	
Cu		− 35.7 [19]	28.4 [19]		− 32.5 [69]	23.53 [31]

larger for $Al_{0.9}Cu_{0.1}$. The opposite is found for D_{Al}, which is smaller than that of pure liquid Al, the difference being larger for $Al_{0.6}Cu_{0.4}$. At the same time, the difference between D_{Al} and D_{Cu} becomes smaller and smaller with increasing Cu composition.

Moreover, we determine that self-diffusion coefficients follow an Arrhenius-type behavior in close agreement with experimental [17,23,24] and theoretical [44,45] values for D_{Cu} for $x \leqslant 0.3$. For $x = 0.4$, we detect a non-Arrhenian behavior below 1200 K. Note that the tendency for an increased non-Arrhenius behavior with increasing Cu content has been reported by Dahlborg *et al.* [23,24]. Calculated activation energies are displayed in Table I, as well as experimental and other theoretical values. The calculated value at $x = 0.4$ is obtained using data corresponding to the Arrhenian dependence of self-diffusion coefficients. We also establish that our calculated values are in the range of the previously reported values.

In Fig. 2(a), we display the evolution of D_{Cu} and D_{Al} as a function of composition for temperatures $T = 1000$, 1400, and 1795 K, and we also compare our data with available experimental data [17,23,24]. We determine that the composition dependence of D_{Cu} and D_{Al} is more pronounced at high temperature than at low temperature. We can mention that the increase of D_{Cu} with increasing Al content is in qualitative agreement with the experimental data of Dahlborg *et al.* [24], and we note that our values of D_{Cu} at $x = 0.2$ are in better agreement with data obtained by Brillo *et al.* [17].

All these results can be related to the occurrence of a chemical short-range order (CSRO), as already discussed for liquid Al-Ni alloys [40,41]. This relation will be discussed further below.

In a second step, we have considered the temperature and composition dependence of the viscosity obtained from the long wavelength limit ($q = 0$) of the q-dependent viscosity given by Eq. (7). As observed for the self-diffusion coefficients, the temperature dependence of the viscosity can be represented by an Arrhenius law in the investigated temperature range for $x \leqslant 0.3$ [see Fig. 1(b)]. For $x = 0.4$, we obtain a non-Arrhenian behavior below 1200 K. Calculated activation energies are reported in Table I for comparison with experimental values. They display a slight linear composition dependence, in agreement with the experimental trend, but the most amazing feature is that they differ strongly from the activation energies found for self-diffusion coefficients.

The composition dependence of the viscosity has been drawn in Fig. 2(b) for temperatures $T = 1000$, 1400, and 1795 K. At high temperatures, our AIMD results are in close agreement with the experimental data [30,31]. At low temperatures, namely at $T = 1000$ K, the agreement is still acceptable, taking into account that the typical experimental error bar is on the order of 10%.

As we dispose of diffusion coefficients and viscosities calculated independently and in agreement with experimental features, we come now to the investigation of the SE relation, in which the ratio $D_i\eta/(k_BT)$ does not depend on temperature. In order to test its validity for the investigated metals and alloys, we plot this ratio as a function of temperature in Fig. 3.

For pure metals, the ratio $D\eta/(k_BT)$ is almost constant, and we find that the effective radius of each metal R_{SE}, is in close agreement with the nearest neighbor distance of metal-metal pairs obtained from experimental or computed pair correlation functions [19,46], as shown in Table II. Then, based on the validity of the SE relation, we can determine diffusivity from viscosity or *vice versa* in pure metals using an effective particle radius taken from the position of the first peak of the pair correlation function.

For alloys with $x = 0.1$ and 0.2, we see that the ratio $D_{Cu}\eta/(k_BT)$ depends on temperature, while $D_{Al}\eta/(k_BT)$ is roughly constant. Note that the temperature dependence of $D_{Cu}\eta/(k_BT)$ is more pronounced at $x = 0.2$. More specifically, we see at this composition that the SE relation breaks down around 1300 K, more than 350 K above the experimental liquidus temperature of these alloys. The breakdown is characterized by an effective SE radius of the copper species, R_{Cu}, which increases with decreasing temperature below 1300 K, becoming larger than the effective radius of pure Cu, as observed experimentally [17].

For $x = 0.3$, the ratio $D_i\eta/(k_BT)$ remains constant within the investigated range of temperatures for the two elements, but the resulting effective SE radii present unreliable values. Indeed, we see from Fig. 4 that the effective SE radius of Cu is larger than that of Al, as well as for other compositions. It is opposite the behavior obtained for pure elements, and we will see in the next paragraph that it is also in contradiction to the structural analysis.

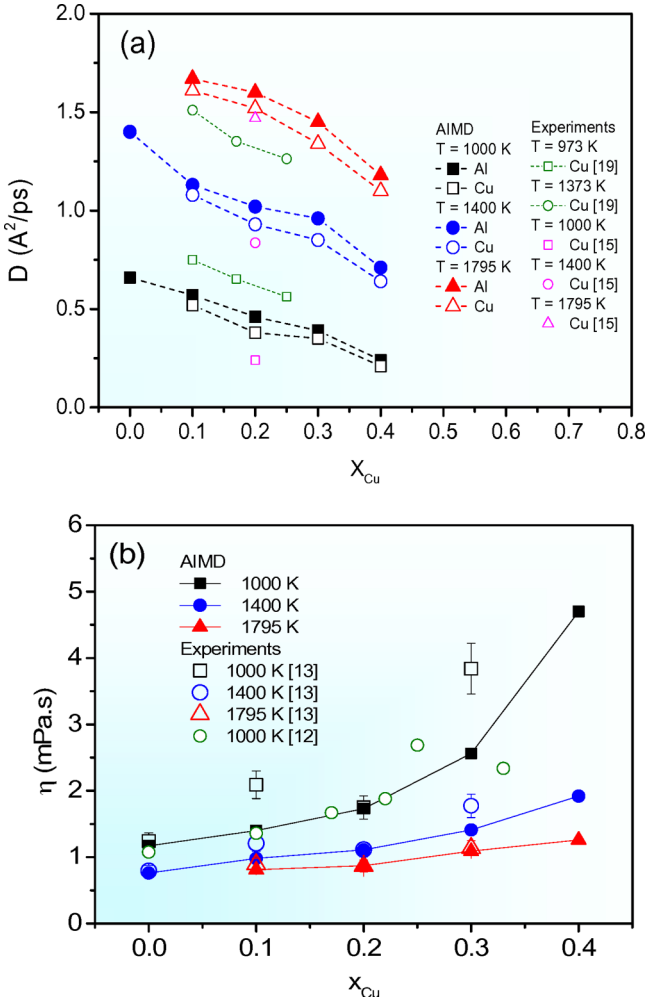

FIG. 2. Composition evolution of calculated (a) Al and Cu self-diffusion coefficients and (b) viscosities. AIMD results for diffusion are compared with the most recent reliable experimental data obtained by quasielastic neutron scattering [17,24]. AIMD results for viscosities are compared with experiments taken from Refs. [30] and [31].

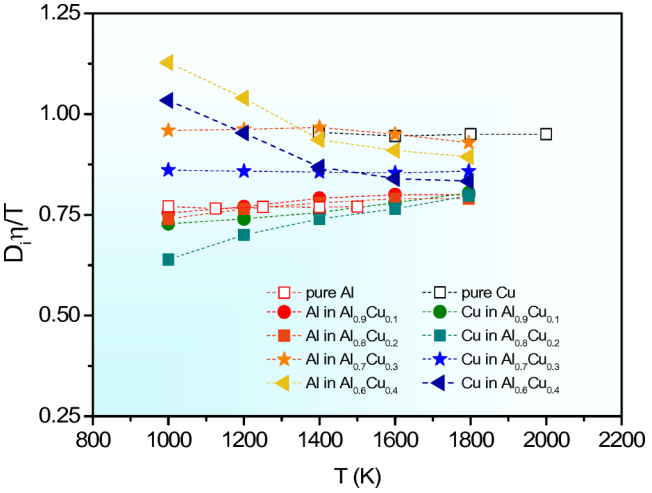

FIG. 3. The ratio $D_i\eta/T$ as a function of temperature for Al-Cu alloys. The corresponding ratio for pure elements Al and Cu are also included.

TABLE II. Atomic diameters R corresponding to the positions of the first maximum of the pair correlation function obtained from *ab initio* molecular dynamics simulations. R_{SE} corresponds to the atomic diameter determined from the Stokes-Einstein relation (see text).

	T (K)	R (Å)	R_{SE}(Å)
Al	1000	2.73	2.84
	1125	2.73	2.80
	1250	2.73	2.82
	1400	2.73	2.86
	1500	2.73	2.85
	1600	2.73	2.86
	1700	2.73	2.88
Cu	1398	2.45	2.30
	1600	2.45	2.32
	1800	2.45	2.34
	2000	2.45	2.34

For $x = 0.4$, we see that both ratios are roughly constant only up to 1300 K and then increase below this temperature. In this case, we suspect that the temperature dependence of both ratios are related to the non-Arrhenian behavior of the self-diffusion coefficients and viscosity.

Therefore, from Fig. 3, we conclude that the temperature dependence of the ratio $D_i\eta/(k_BT)$ is composition dependent in liquid $Al_{1-x}Cu_x$ alloys. We also find that both R_{SE}^{Cu} and R_{SE}^{Al} display at low temperature a strong composition dependence and that R_{SE}^{Cu} is always larger than R_{SE}^{Al} within the investigated composition range. This will be examined in more detail in the following section. Finally, we suspect the non-Arrhenian behavior of transport properties at $x = 0.4$ is the origin of the breakdown of the SE relation in this composition.

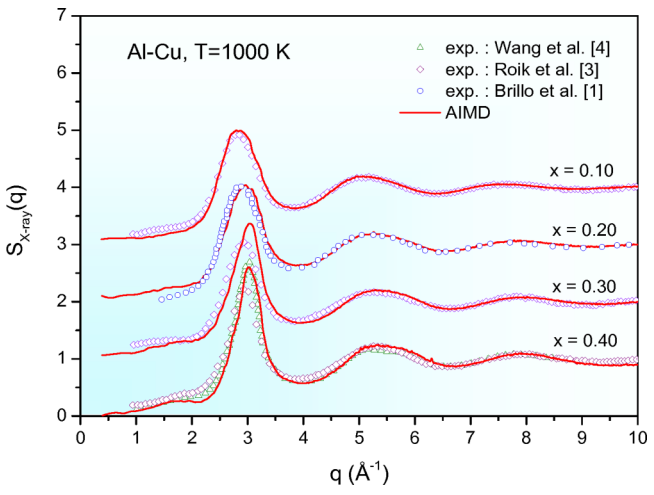

FIG. 4. Total x-ray structure factor for composition $x = 0.1$, $x = 0.2$, $x = 0.3$, and $x = 0.4$ at $T = 1000$ K and compared with experimental curves, respectively, for $x = 0.14$ [48], $x = 0.17$ [47], $x = 0.3$ [48], and $x = 0.4$ [45,48]. The experimental temperatures of Ref. [48] are 50 K above the liquidus temperature, and that of Ref. [47] is 1023 K. The curves for $x = 0.3$, $x = 0.2$, and $x = 0.1$ are shifted upward by an amount of 1, 2, and 3, respectively.

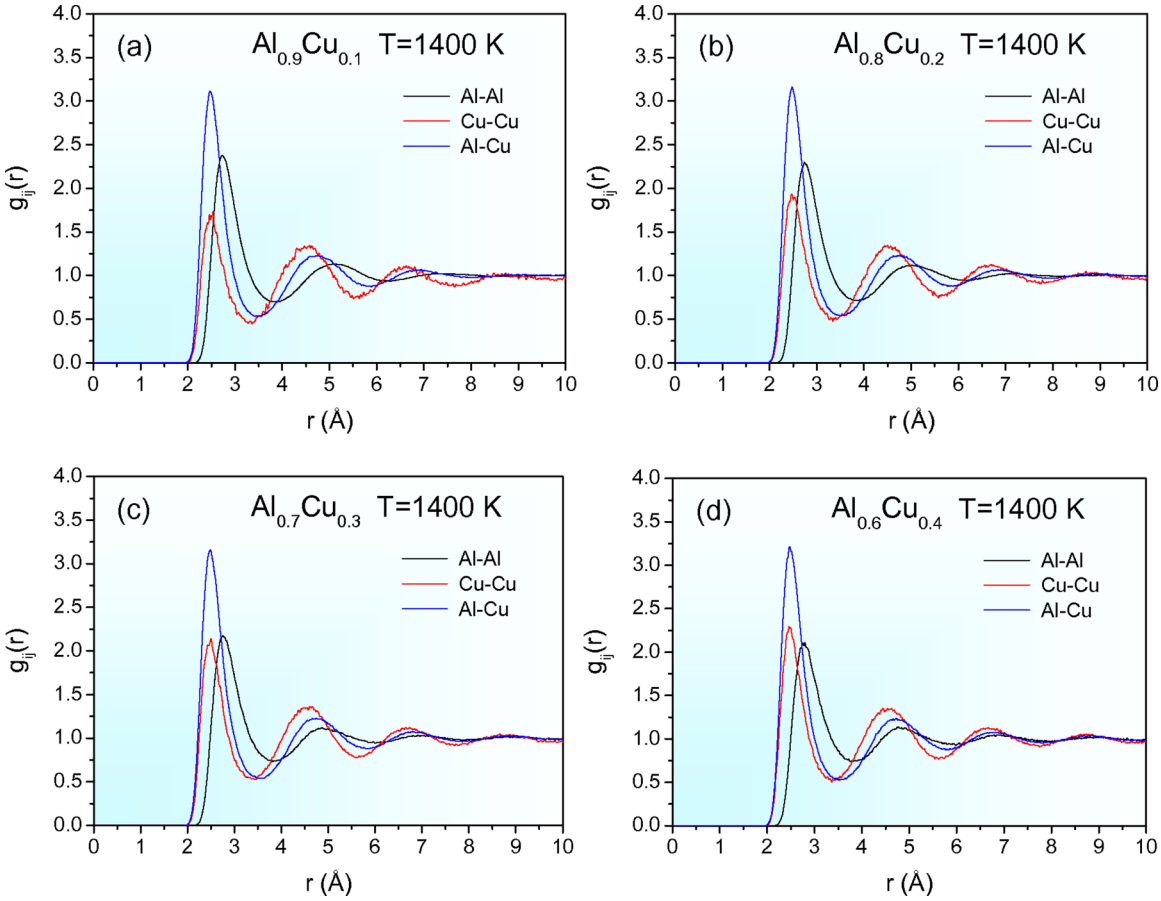

FIG. 5. Partial-pair correlation functions for Al-Cu alloys at temperature $T = 1400$ K, for composition (a) $x = 0.1$, (b) $x = 0.2$, (c) $x = 0.3$, and (d) $x = 0.4$.

B. Local ordering of $Al_{1-x}Cu_x$ alloys

To go further into understanding the temperature and composition dependence of the transport properties of $Al_{1-x}Cu_x$ alloys, we proceed to the analysis of their local ordering through (i) partial-pair correlation functions and (ii) the common neighbor indexation to obtain a detailed 3D picture of the topology surrounding each chemical species.

Before analyzing the partial-pair correlation functions, we first display in Fig. 4 the corresponding total structure factors for x-ray diffraction at $T = 1000$ K. They are compared with existing experimental data in Refs. [45,47], and [48], and for all compositions, good agreement guarantees the validity of our simulations.

We show now partial-pair correlation functions, $g_{\mathrm{AlAl}}(r)$, $g_{\mathrm{AlCu}}(r)$, and $g_{\mathrm{CuCu}}(r)$ in Figs. 5(a)–5(d), respectively, for $x = 0.1$, 0.2, 0.3, and 0.4. Our results indicate that changes with temperature are small regarding amplitudes and peak positions, whatever the composition. Therefore, we report our results only for one temperature located in the middle of the investigated range of each composition, namely 1400 K.

As the Cu concentration increases, the first peak of the Al-Al partial decreases, and its position shifts slightly toward larger distances, while that of the Cu-Cu partial increases, and its position slightly moves toward smaller distances. In Fig. 6, we report the position of the first peaks of these two partials as a function of composition for comparison with the values of $R_{\mathrm{SE}}^{\mathrm{Al}}$ and $R_{\mathrm{SE}}^{\mathrm{Cu}}$ obtained at high and low temperature, i.e., 1795 and 1000 K, respectively. We can see that the relative position of the first peaks of $g_{\mathrm{AlAl}}(r)$ and $g_{\mathrm{CuCu}}(r)$ is in contradiction with the fact that the effective radius for Cu species is higher than

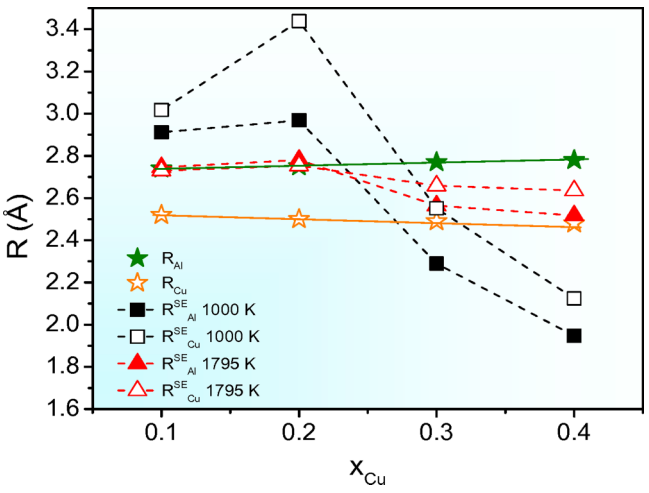

FIG. 6. Radii of the species as a function of copper composition for temperature $T = 1400$ K determined from the partial-pair correlation function. They are compared with the effective Stokes-Einstein radii at temperatures $T = 1000$ K and $T = 1795$ K.

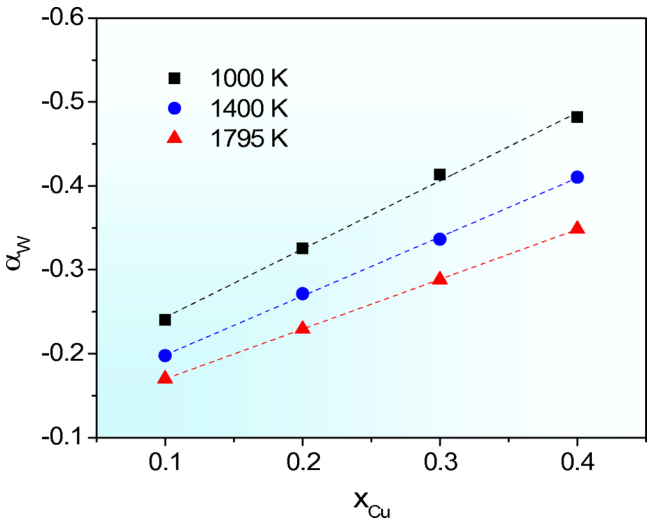

FIG. 7. Warren-Cowley parameter as a function of copper composition for temperatures $T = 1000$ K, $T = 1400$ K, and $T = 1795$ K.

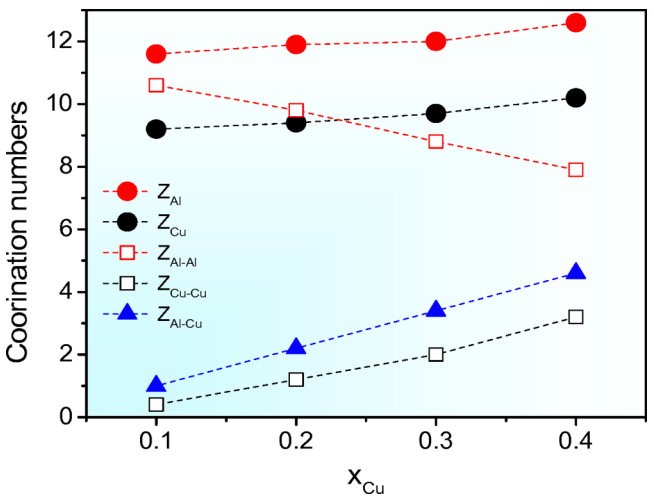

FIG. 8. Total and partial coordination numbers as a function of copper composition for temperature $T = 1400$ K.

that of Al species, as obtained from $D_i\eta/(k_BT)$. Therefore, we cannot use interatomic distances of liquid alloys from the partial-pair correlation functions to determine effective radii for both elements to be inserted in the SE relation. We also mention that we cannot identify the effective SE radius of the copper species to the position of the first peak of the Cu-Cu pair correlation function to interpret the temperature dependence of the ratio $D_{Cu}\eta/(k_BT)$ for $Al_{1-x}Cu_x$ alloys with $x = 0.1$, 0.2, and 0.4.

Another point is the amplitude of the first peak of $g_{AlCu}(r)$ which is larger with respect to the two other partials, whatever the composition. Such behavior indicates a hetero-coordination in the alloy with preferred Al-Cu bonds, leading to the occurrence of a CSRO. To determine the CSRO more quantitatively, we use the Warren order parameter, i.e., $\alpha_W = 1 - Z_{CuAl}/x_{Al}(x_{Cu}Z_{Al} - x_{Al}Z_{Cu})$, where Z_{CuAl} is the partial coordination number, Z_{Al} and Z_{Cu} are the total coordination numbers around Al and Cu atoms, and x_{Al} and x_{Cu} are the partial concentrations of the corresponding species. Note that coordination numbers describing the number of j-type atoms around i-type atoms within the first nearest neighbor shell are obtained by integrating computed partial-pair correlation functions up to their first minima.

We report in Fig. 7 results obtained for the computed values of α obtained for the different alloys as a function of composition and for various temperatures. For all investigated alloys, it takes negative values, which confirms quantitatively a preference for hetero-atomic bonds. Note that CSRO increases linearly with composition. We think this CSRO favors the observed similarity of diffusion coefficients of the two species.

Coordination numbers can also be used directly as structural indicators, in relation to the cage effect, which is the main mechanism used to interpret the atomic diffusion in metallic systems [49]. We show in Fig. 8 results as a function of composition for the intermediate temperature $T = 1400$ K. For Al atoms, we find that the total coordination number z_{Al} varies from 11.5 to 12.5, while the total coordination around Cu atoms, z_{Cu}, varies from 9.2 to 10.2. From these data, we do not find any correlation, since the difference between coordination numbers of Al and Cu is roughly constant, while the two species display closer and closer diffusivities with increasing Cu composition. Therefore, we have to proceed to a more detailed description of local ordering.

To obtain a deeper insight into the evolution of local ordering as a function of the composition, we can use the CNA [41], as already performed in liquid $Al_{1-x}Ni_x$ alloys [42,43]. In Fig. 9, we display the temperature evolution of the main bonded pairs for $Al_{1-x}Cu_x$ alloys, as well as for pure liquid Al and Cu. The number of 15xx, namely the 1551, 1541, and 1431 bonded pairs, is a direct measure of the degree of icosahedral ordering, including both perfect and distorted icosahedral motifs, as already used in other theoretical studies [50,51]. The number of the 142x(1422 + 1421) bonded pairs is characteristic of close packed structures, while the 1311 and the 1321 bonded pairs are related to disorderly structures.

For pure aluminum and copper, we first observe at high temperatures that the CNA yields a different local ordering, since the abundance of 15xx pairs is much more important (by a factor two) in Cu than in Al, while we observe the opposite for the 142x and 131x pairs. During cooling, the total fraction of icosahedral-like motifs increases greatly, while the fraction of disordered 13xx(1311 + 1321)-type pairs decreases for both species. We note that during cooling, the fraction of 142x bonded pairs also increases, but only slightly. It might be reasonable to speculate that liquid Al and Cu display a more important local ordering when decreasing the temperature in their liquid phase, and the local ordering around each species remains quite different. We observe the same trend for $Al_{1-x}Cu_x$ alloys upon cooling, but the most striking result is the significant increase of icosahedral ordering around Al atoms with increasing Cu content, even at high temperature, while we observe a slight decrease of icosahedral ordering around Cu atoms. As a consequence, local structures around each species, as defined by CNA, become closer and closer with increasing Cu content, mainly due to a favorable interplay between ISRO and CSRO. Another consequence is that local structures around Al and Cu atoms also display a similar evolution as a function of temperature for $x \geqslant 0.3$. Note that this trend can be also correlated with the composition

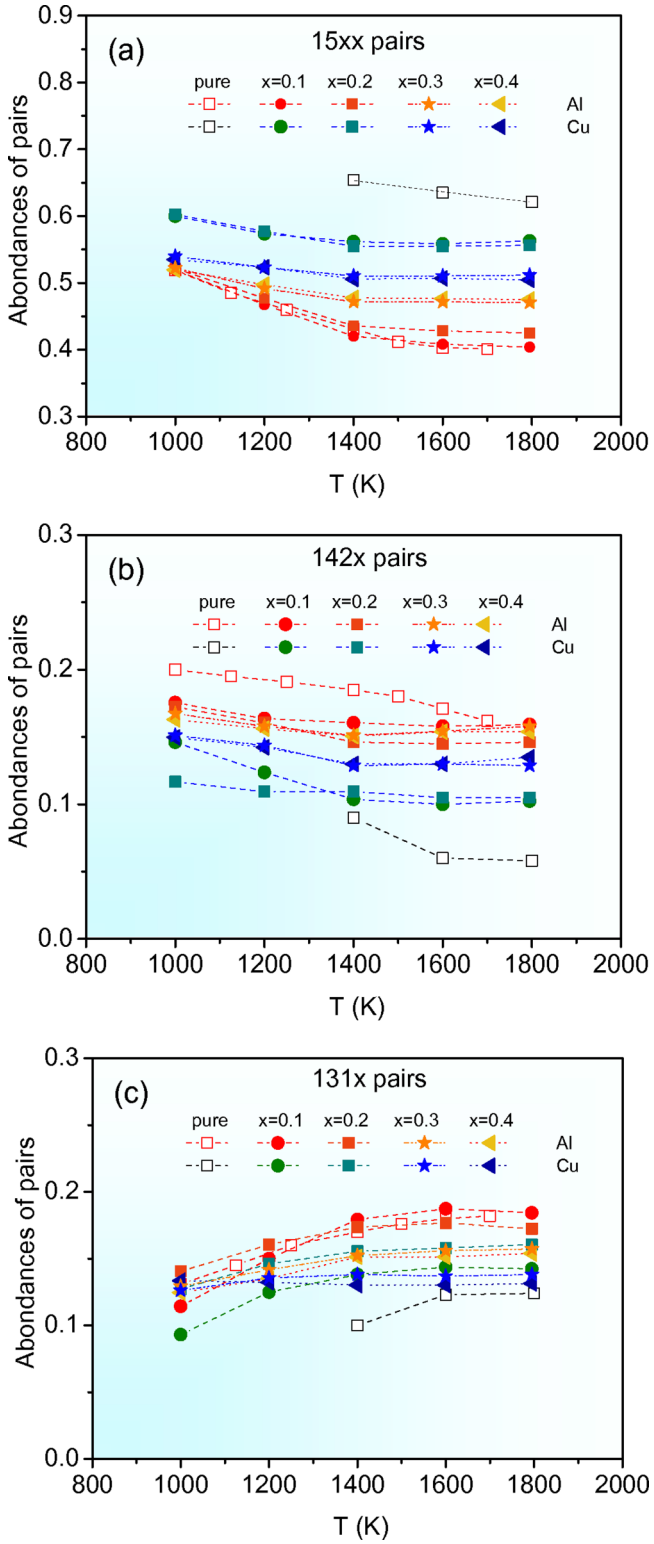

FIG. 9. Abundances of pairs as a function of temperature for Al-Cu alloys obtained from common neighbor analysis around Al and Cu atoms: (a) 15xx(1551 + 1541 + 1431) bonded pairs, (b) 142x(1422 + 1421) bonded pairs, and (c) 13xx(1311 + 1321) bonded pairs. Results for pure Al and Cu are included. The error bars are on the order of 0.01.

dependence of D_{Al} and D_{Cu}, since the difference between D_{Al} and D_{Cu} becomes smaller and smaller with increasing Cu composition, as described above. The underlying mechanism could be that icosahedral motifs are known to be the most compact local structures and therefore correspond to the most important cage effect [49]. As a consequence, the backscattering regime is more pronounced for species that display the highest ISRO, and their diffusivity is smaller. As the degree of ISRO for Al and Cu species becomes closer and closer, D_{Al} and D_{Cu} follow the same trend. Note that the correlation between ISRO and the viscosity of investigated $Al_{1-x}Cu_x$ alloys is also clear, in agreement with the discussion in Ref. [52], stating that the more important the IRSO, the more important the viscosity.

The same argument holds to describe the temperature dependence of D_{Al} and D_{Cu} (which is quite different for low-Cu compositions), as well as the temperature evolution of the degree of ISRO around Al and Cu species. It is particularly true for $x = 0.2$, as seen from Fig. 1. Below 1400 K, we observe decoupling of the diffusion of both species, here referred to as chemically induced decoupling [21]. Such a decoupling leads to the breakdown of the SE relation for Cu, the minority element. To conclude our discussion, we mention that other microscopic mechanisms are proposed in the literature to explain this decoupling, like the model of local configuration excitations in the atomic connectivity network proposed by Egami and coworkers [53]. In these terms, Cu atoms would form stronger temporary nearest neighbor bonds compared with Al atoms. Such a behavior can be connected to the preferential icosahedral symmetry around Cu atoms [54]. Another approach is based on the self-hole filling dynamics, as proposed by Han *et al.* [12] to interpret the high-temperature breakdown of the SE relation found in liquids Cu_8Zr_3 and $CuZr_2$. Within this scheme, the onset of the breakdown of the SE relation corresponds also to a critical temperature from which the viscosity of these liquids begins to deviate from its higher temperature Arrhenius behavior. Because the viscosity of liquid $Al_{0.8}Cu_{0.2}$ follows an Arrhenius behavior in the investigated temperature range, it seems difficult to connect our results with this approach.

C. Structural entropy and Rosenfeld's scaling laws

In a recent contribution [43,55], we have revealed a strong correlation between the composition dependence of the local ordering of liquid $Al_{1-x}Ni_x$ alloys and the partial structural or pair excess entropy [32,33], which can be obtained for a binary alloy in terms of the partial-pair correlation functions,

$$S_2 = -2\pi\rho \sum_{i,j=1}^{N} x_i x_j \int_0^\infty \{g_{ij}(r)\ln[g_{ij}(r)] - [g_{ij}(r) - 1]\} r^2 dr$$

$$= \sum_{i=1}^{2} x_i S_2^i, \qquad (9)$$

ρ being the number density and the composition of species i.

In Fig. 10, we plot partial (S_2^i) and total structural entropies (S_2) as a function of inverse temperature for $Al_{1-x}Cu_x$ alloys. We note a significant variation of S_2 and S_2^i as a function of composition for Al-Cu alloys, which is consistent with the evolution of local ordering as discussed above. All quantities display lower values with increasing Cu concentration when

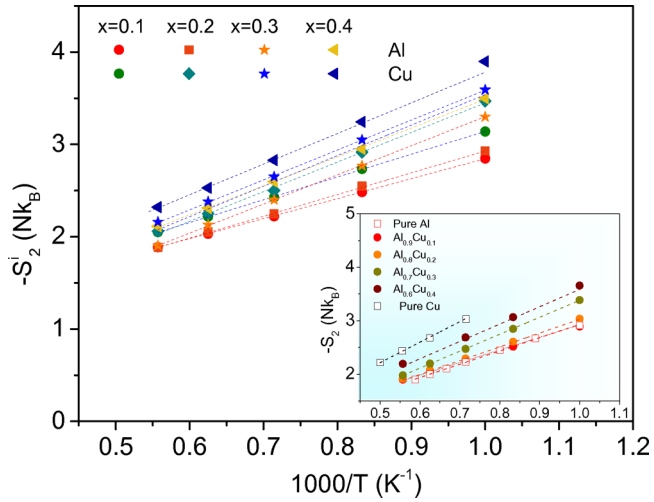

FIG. 10. Inverse temperature dependence of the structural entropy for all Al-Cu alloys. The inset shows the inverse temperature dependence of the total structural entropy for all Al-Cu alloys, as well as that for pure Al and Cu liquids.

ISRO and CSRO also increase. We note also that partial excess entropies S_2^{Al} and S_2^{Cu}, display a quasi "near parallel" behavior as a function of temperature for $x = 0.3$ and $x = 0.4$ but, in this case, only for $T \geqslant 1300$ K, in close correspondence with the similar temperature dependence of local ordering found for these two compositions. To quantify the ability of S_2 to be used in a relationship with transport properties, we plot self-diffusion coefficients and viscosity of each alloy as a function of S_2 in Fig. 11 within the investigated range of temperatures. We can see that both the self-diffusivity and viscosity show strong couplings to static structure via S_2. Therefore, the structural entropy computed from pair correlation functions appears to act as a structural indicator to measure the local ordering in liquid $\mathrm{Al}_{1-x}\mathrm{Cu}_x$ alloys, as well to provide good correlation with their transport properties.

Whether structural entropy can be used to interpret the temperature dependence of the ratio $D_i\eta/(k_BT)$ and the breakdown of the Stokes-Einstein equation found in some of these alloys is an important question, which merits discussion.

To make a more quantitative link between structural entropy and dynamic properties, we consider its relation to transport properties via entropy-scaling laws [56,57]. More specifically, we make use of the semiquantitative correlation proposed by Rosenfeld [56]. To our best knowledge, Rosenfeld's scheme is the only one that treats the scaling laws for diffusion and viscosity on the same footing, which is a prerequisite for supporting our considerations. Rosenfeld asserts that a reduced coefficient of self-diffusion D^* and the reduced viscosity η^* can be expressed as a function of S_{ex},

$$D^* = D\frac{\rho^{1/3}}{(k_BT/m)^{1/2}} = A\exp(\alpha S_{\mathrm{ex}}), \tag{10}$$

$$\eta^* = \eta\frac{\rho^{-2/3}}{(mk_BT)^{1/2}} = B\exp(-\beta S_{\mathrm{ex}}), \tag{11}$$

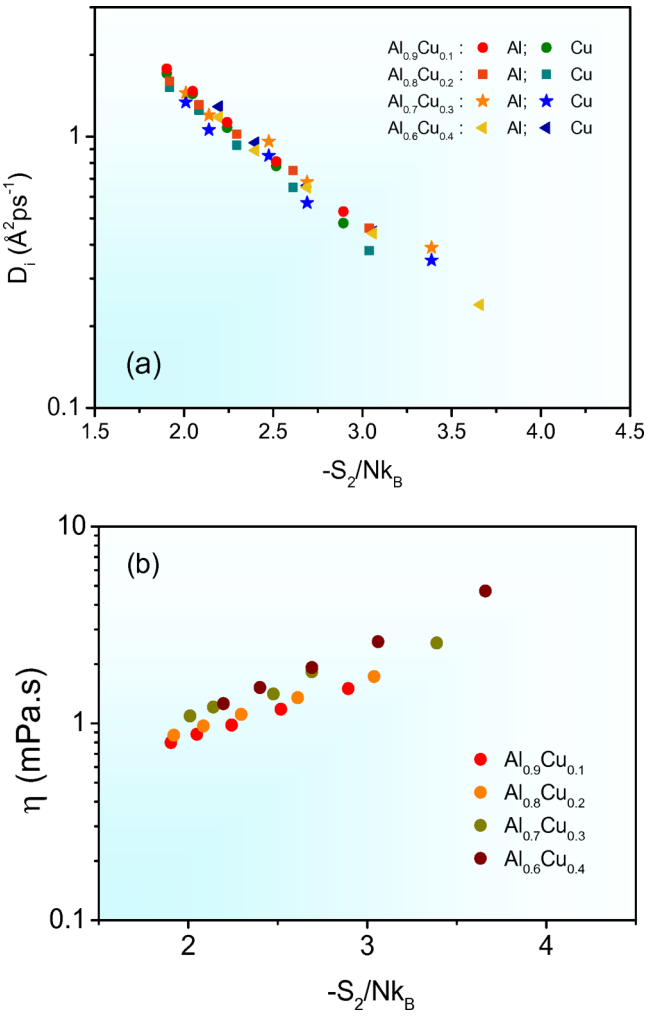

FIG. 11. Calculated self-diffusion coefficients of Al and Cu species (a) and viscosities (b) as a function of total structural entropy for all Al-Cu alloys and all temperatures in the semilog scale.

where ρ is the number density, and m is the atomic mass. A, B, α, and β are property-specific constants equal to 0.6, 0.2, 0.8, and 0.8, respectively, for model fluids [56].

Many studies [57–65] in which S_{ex} is most often replaced by S_2, have shown that these entropy-scaling laws provide a quantitative connection between diffusivity and local structural ordering, even for melts described by realistic many-body potentials [59,60] or using *ab initio* calculations [19].

Here, we adopt a different strategy by using Eqs. (10) and (11) and S_2 to reformulate the SE equation. For a simple liquid, we obtain:

$$D\eta/(k_BT) \sim \rho^{1/3}\exp[(\alpha-\beta)S_2] \tag{12}$$

The radius of the particle used in the familiar expression of the SE relation, which is equal to $k_BT/C\pi\eta D$, can be related here to ρ; namely, $R = 0.5\rho^{-1/3}$. Then, Eq. (12) indicates that the SE relation holds only if the term $\exp((\alpha-\beta)S_2)$ does not depend on temperature. As S_2 varies with temperature, as shown in Fig. 10 and in Ref. [60], α must be equal to β. Note that this condition is satisfied in Rosenfeld's assessment for model fluids, as mentioned above.

For a liquid alloy, we have to take into account that the reduced viscosity is expressed as a function of S_2, while the diffusion coefficient of the i species depends only on S_2^i. In this case, the SE relation for each species i is given by:

$$\frac{D_i \eta}{k_B T} \sim \rho^{1/3} \exp\left(\alpha_i S_2^i - \beta S_2\right). \tag{13}$$

Equation (13) evidences that partial and total structural entropies and their evolution as a function of temperature play a key role in understanding the validity of the SE relation, in addition to the α_i and β parameters.

To check the assumptions used in Eqs. (10) and (11), we first plot the reduced self-diffusion coefficient and reduced viscosity as a function of the structural entropy for pure Al and Cu liquids, as well as for $Al_{1-x}Cu_x$ alloys in Figs. 12(a) and 12(b), respectively. We can see that for both elements, we obtain a similar slope for reduced self-diffusion and viscosity; namely, $\alpha = \beta = 0.9$ with an uncertainty of ± 0.03. This value corresponds to the slope of the dashed lines in Figs. 12(a) and 12(b). It is interesting to note that this value obtained for "real"

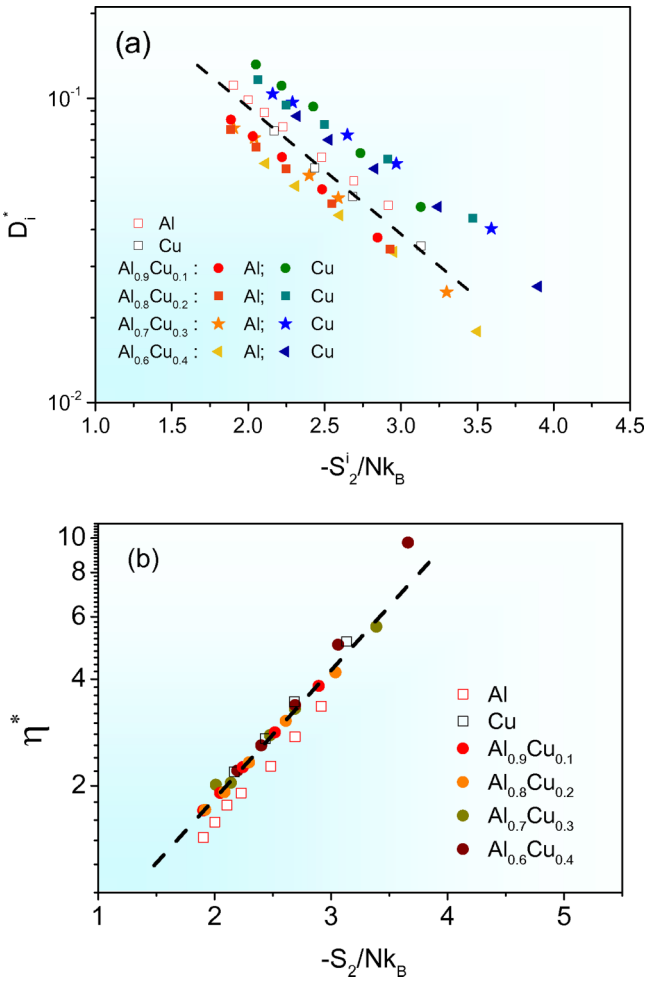

FIG. 12. Rosenfeld's scaling law with the structural entropy for liquid metals and alloys: (a) reduced diffusion D^* as a function of the partial two-body entropy S_2. (b) Reduced viscosity η^* as a function of the two-body entropy S_2.

liquids described by AIMD simulations is close to that used in Rosenfeld's original work for model fluids.

For $Al_{1-x}Cu_x$ alloys, we find that reduced diffusivities of Al of all investigated alloys, D^*_{Al}, display a slope of 0.9 similar to that of pure metals, while it is also true for the reduced diffusivity of Cu, D^*_{Cu}, at $x = 0.1$. For other compositions, D^*_{Cu} presents a weaker slope, namely $\alpha_{Cu} = 0.85$, which is, however, not so far from 0.9. Finally, we observe that reduced viscosities of all investigated alloys, except $x = 0.4$, display the same slope as that found for pure metals, i.e., $\beta = 0.9$. For $x = 0.4$, we notice that reduced viscosities depart from the dashed line at low temperatures, namely below 1200 K. We will turn back to this behavior later.

To test conclusions obtained from Eqs. (12) and (13), we plot the quantity $\exp(\alpha_i S_2^i - \beta S_2)$ for $Al_{1-x}Cu_x$ alloys as a function of temperature in Figs. 13(a)–13(d). By comparing with Fig. 4, we find that $\exp(\alpha_i S_2^i - \beta S_2)$ correlates pretty well with the ratio $D_i\eta/(k_B T)$, except for $D_{Cu}\eta/(k_B T)$ at $x = 0.4$. More specifically, the quantity $\exp(\alpha_i S_2^i - \beta S_2)$ describes correctly the temperature dependence of the ratio $D_i\eta/(k_B T)$ and the hierarchy between the self-diffusion coefficients in all investigated alloys with $x = 0.1$, 0.2, and 0.3; that is, self-diffusions of Cu are found to be smaller than the self-diffusion of Al in Al-Cu alloys.

For $x = 0.4$, we obtain also the correct hierarchy, but the quantity $\exp(\alpha_{Cu} S_2^{Cu} - \beta S_2)$ is not able to reproduce the temperature dependence of $D_{Cu}\eta/(k_B T)$. For this composition, we suspect that the crossover from Arrhenius to non-Arrhenius temperature evolution of diffusivity and viscosity starting around 1300 K to be the origin of this failure. As this crossover is often attributed to dynamic heterogeneities usually observed in the supercooled regime, it is necessary to establish the existence of DHs, or not, at a temperature located only 150 K higher than the experimental liquidus temperature. The DH can be quantified by means of the non-Gaussian parameter [66] defined as

$$\alpha_2(t) = 3R^4(t)/5[R^2(t)]^2 - 1, \tag{14}$$

where $R^2(t)$ and $R^4(t)$ are, respectively, the mean square displacement given by Eq. (1) and mean quadruple displacement. Typically, $\alpha_2(t)$ reaches a maximum value α_2^{max} around 0.2 on the subpicosecond scale due to the anisotropy of atomic motions in the ballistic regime. Then, a rapid decrease toward zero, inversely proportional to time, is observed at long time periods, which is an indication of a homogeneous diffusive regime. Otherwise, an increase of the amplitude of α_2^{max} above 0.2 is associated with an increasing degree of DH.

We have drawn the curves of $\alpha_2(t)$ for $x = 0.4$ at temperatures $T = 1000$, 1400, and 1795 K, respectively, for Al and Cu in Fig. 14. At high temperature, namely $T = 1795$ K, only a weak maximum is observed, which is characteristic of a homogeneous diffusion regime. As the temperature decreases down to $T = 1400$ K, we observe only a small increase of α_2^{max} with a position remaining on the subpicosecond time scale, revealing only a small degree of DH. Homogeneous diffusion is restored on a picosecond time scale. Below $T = 1400$ K and up to 1000 K, we observe a rapid increase of α_2^{max}, indicating a pronounced degree of DH that grows and occurs later and later with decreasing temperature. We notice that the amplitude of α_2^{max} becomes higher for Cu than for Al. Therefore DHs are

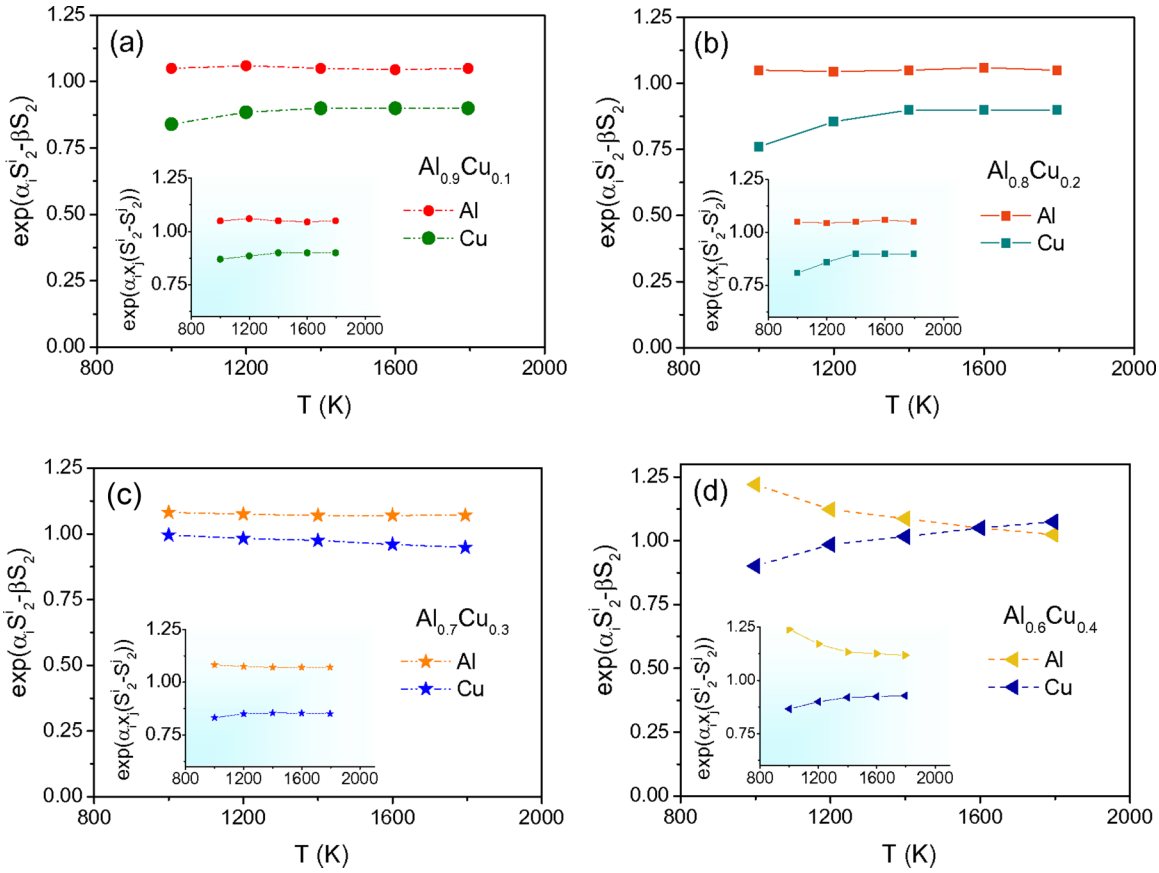

FIG. 13. Quantity $\exp(\alpha_i S_2^i - \beta S_2)$ as a function of temperature for composition (a) $x = 0.1$, (b) $x = 0.2$, (c) $x = 0.3$, and (d) $x = 0.4$. The corresponding insets display the quantity $\exp(\alpha_i x_j (S_2^i - S_2^j))$ as a function of temperature (see text).

at the origin of the breakdown of the SE equation for the $Al_{0.6}Cu_{0.4}$ melt slightly above the liquidus temperature. Note that a similar result was obtained for the Cu_8Zr_3 melt [12].

To go further in the predictive character of Eq. (13), we state that the Rosenfeld scaling law holds reasonably well for $Al_{1-x}Cu_x$ alloys with $\alpha_i = \alpha_j = \alpha = \beta$. In this case, the quantity $\exp(\alpha_i S_2^i - \beta S_2)$ can be rewritten like $\exp(\alpha(S_2^i - S_2))$ or $\exp(\alpha x_j (S_2^i - S_2^j))$, where x_j is the composition of j species in the alloy. We point out that this term does not vary with temperature only if S_2^i and S_2^j display the same temperature dependence. As a matter of fact, we obtain from Fig. 11 that S_2^{Al} and S_2^{Cu} display a "near parallel" behavior only for $x = 0.3$ and for $x = 0.4$ up to 1300 K. Below this temperature, we observe a change in the slope of both partial structural entropies. Then we can conclude that the "near parallel" character of partial structural entropies can be used to predict, at least qualitatively, the constant behavior of the ratio $D_i\eta/(k_B T)$ with temperature.

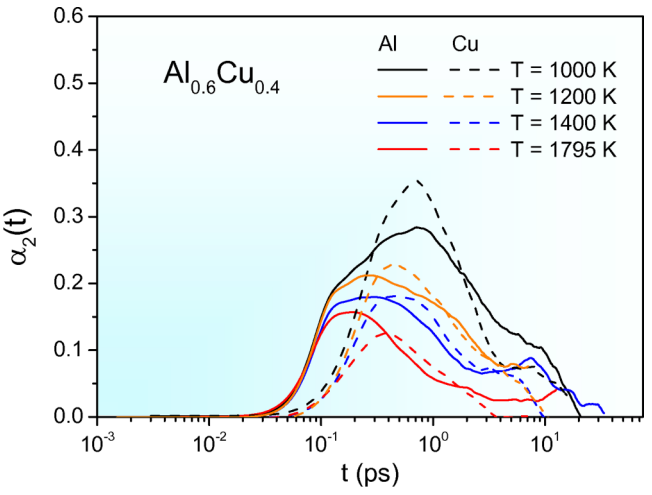

FIG. 14. Non-Gaussian parameter of Al and Cu species as a function of time for composition $x = 0.4$ and for various temperatures.

We also mention that the "nonparallel" temperature evolution of partial structural entropies has a stronger impact on Cu than on Al, because the impact of alloying effects on local ordering is more important for the minority constituent, namely for Cu at $x_{Cu} = 0.1$ and 0.2. This is also highlighted in the quantity $\exp(\alpha x_j (S_2^i - S_2^j))$, in which the difference $(S_2^i - S_2^j)$ is multiplied either by x_{Al}, equal to 0.9 or 0.8, to determine the temperature dependence of $D_{Cu}\eta/(k_B T)$ or by x_{Cu}, equal to 0.1 or 0.2, for $D_{Al}\eta/(k_B T)$.

The last point concerns the hierarchy between the self-diffusion coefficients in a given alloy. From Eq. (13), we obtain the ratio D_i/D_j as a function of $\exp(\alpha_i S_2^i - \alpha_j S_2^j)$. As discussed above, α_i is roughly equal to α_j and assuming that $\alpha(S_2^i - S_2^j)$ is small, we can approximate D_i/D_j by the ratio

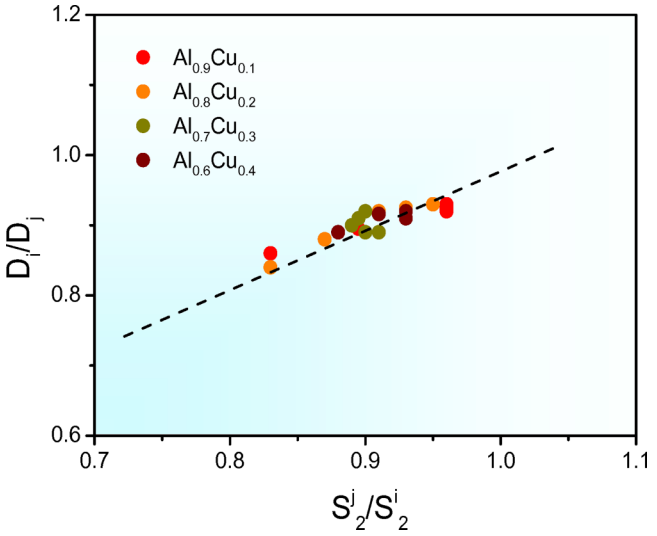

FIG. 15. Self-diffusion ratio D_i/D_j of Al and Cu species as a function of the partial entropy ratio S_2^j/S_2^i for all compositions.

of partial excess entropies S_2^j/S_2^i. Indeed, Fig. 15 shows that both quantities correlate very well. Our findings may help in determining easily the full set of self-diffusion coefficients of constituents in an alloy using macroscopic quantities readily obtainable from standard experiments and simulations. The peculiar case of Al-based alloys is mainly of interest, as the accurate determination of self-diffusion coefficients of elements like Al is an experimentally difficult task [67,68].

IV. CONCLUSION

In summary, we have used *ab initio* molecular dynamics simulations to study structural and dynamic properties of liquid $Al_{1-x}Cu_x$ alloys.

First, we determine that self-diffusion coefficients and viscosity of these liquids display a monotonous composition dependence within the investigated concentration range, while their temperature dependence follows an Arrhenius-type behavior, except for $x = 0.4$ at low temperatures.

Second, we evidence a strong evolution of local structural ordering around each species as a function of composition, characterized by an increase of interplay between CSRO and ISRO that depends on composition and temperature. On one side, we show that such a local ordering cannot be captured by composition and temperature evolution of the interatomic distances found in liquid phases. This can explain the inability of the SE relation to describe the relationship between diffusivity and viscosity using effective diameters of Al and Cu atoms taken from them. On the other hand, we demonstrate that the partial structural entropies for Al and Cu atoms are indicators to establish a clear correlation between local ordering and transport properties in liquid $Al_{1-x}Cu_x$ alloys.

All these findings lead us to propose an approach to describe transport properties of metallic liquids using AIMD simulations on the basis of Rosenfeld's scaling law and partial structural entropies. More specifically, we show that the breakdown of the SE relation in the liquid regime can be related to the "nonparallel" behavior of partial structural entropies when transport properties display an Arrhenius-type behavior. This "nonparallel" behavior can be related to the nonsimilarity of local ordering around Al and Cu species at low Cu composition. For $x = 0.4$, we obtain that dynamic heterogeneities are at the origin of the breakdown of the SE relation, even in the liquid phase, and are characterized by a change in the slope of both partial structural entropies.

We also derive a simple relation between the ratio of self-diffusivities of the two components and the ratio of their corresponding pair partial structural entropies. In the peculiar case of Al-based alloys, it is of primary interest because the accurate determination of self-diffusion coefficients of elements like Al is an experimentally difficult task.

We think that our findings will trigger more experimental and theoretical studies, since structural entropies used in the present paper to discuss the applicability of the SE equation are easily obtained from standard experiments and simulations.

ACKNOWLEDGMENTS

We thank Jürgen Brillo, Andreas Meyer, and Thomas Voigtman for fruitful discussions. We acknowledge the Centre Informatique National de l'Enseignement Supérieur (CINES) and Institut du Développement et des Ressources en Informatique Scientifique (IDRIS) under Project No. INP2227/72914, as well as PHYNUM CIMENT for computational resources. This work was performed within the framework of the Centre of Excellence of Multifunctional Architectured Materials (CEMAM) No. ANR-10-LABX-44-01 funded by the "Investments for the Future" program.

[1] J. P. Hansen and I. R. McDonald, *Theory of Simple Liquids* (Academic, London, 1986).
[2] J. Jonas and J. A. Akai, J. Phys. Chem. **66**, 4946 (1977).
[3] N. Jakse and A. Pasturel, J. Chem. Phys. **144**, 244502 (2016).
[4] M. D. Ediger, P. Harrowell, and L. Yu, J. Chem. Phys. **128**, 034709 (2008).
[5] K. L. Ngai, J. H. Magill, and D. J. Plazek, J. Chem. Phys. **112**, 1887 (2000).
[6] T. Wu and L. Yu, J. Phys. Chem. B **110**, 15694 (2006).
[7] L. Berthier and G. Biroli, Rev. Mod. Phys. **83**, 587 (2011).
[8] M. D. Ediger, J. Phys. Chem. **100**, 13200 (1996).
[9] J. F. Douglas and D. Leporini, J. Non-Cryst. Solids **235–237**, 137 (1998).
[10] A. Jaiswal, T. Egami, and Y. Zhang, Phys. Rev. B **91**, 134204 (2015).
[11] P. Bordat, F. Affouard, M. Descamps, and F. Müller-Plathe, J. Phys. Condens. Matter **15**, 5397 (2003).
[12] X. J. Han and H. R. Schober, Phys. Rev. B **83**, 224201 (2011); X. J. Han, J. G. Li, and H. R. Schober, J. Chem. Phys. **144**, 124505 (2016).
[13] A. C. Pan, J. P. Garrahan, and D. Chandler, Phys. Rev. E **72**, 041106 (2005).

[14] K. Lad, N. Jakse, and A. Paaturel, J. Chem. Phys. **136**, 104509 (2012).
[15] S. M. Chathoth and K. Samwer, Appl. Phys. Lett. **97**, 221910 (2010).
[16] J. Brillo, *Thermodynamics Properties of Multicomponent Liquid Alloys* (De Gruyter, Germany, 2016).
[17] J. Brillo, S. M. Chathoth, M. M. Koza, and A. Meyer, Appl. Phys. Lett. **93**, 121905 (2008).
[18] J. Brillo, A. I. Pommrich, and A. Meyer, Phys. Rev. Lett. **107**, 165902 (2011).
[19] N. Jakse and A. Pasturel, Sci. Rep. (Nature) **6**, 20689 (2016).
[20] N. Jakse, O. Lebacq, and A. Pasturel, Phys. Rev. Lett. **93**, 207801 (2004); J. Chem. Phys. **123**, 104508 (2005).
[21] M. D. Ediger and P. Harrowell, J. Chem. Phys. **137**, 080901 (2012).
[22] M. Maret, T. Pomme, A. Pasturel, and P. Chieux, Phys. Rev. B **42**, 1598 (1990).
[23] U. Dahlborg, M. Besser, M. Calvo-Dahlborg, S. Janssen, F. Juranyi, M. J. Kramer, J. P. Morris, and D. J. Sordelet, J. Non-Cryst. Solids **353**, 3295 (2007).
[24] U. Dahlborg, M. Besser, M. J. Kramer, J. R. Morris, and M. Calvo-Dahlborg, Physica B **412**, 50 (2013).
[25] A. M. Korol'kov, *Casting Properties of Metals and Alloys*, (Consultants Bureau, New York, NY, 1960), p. 64.
[26] E. Gebhardt, M. Becker, and S. Dorner, Aluminium **31**, 315 (1955).
[27] F. Lihl, E. Nachtigall, and A. Schwaiger, Z. Metallkunde **59**, 213 (1968).
[28] H. A. Friedrichs, L. W. Ronkow, and Y. Zhou, Steel Res **68**, 209 (1997).
[29] Y. Plevachuk, V. Sklyarchuk, A. Yakymovych, S. Eckert, B. Willers, and K. Eignefled, Met. Mater. Trans. A **39**, 3040 (2008).
[30] N. Yu. Konstantinova, P. S. Popel, and D. A. Yagodin, High Temp. **47**, 336 (2009).
[31] M. Schick, J. Brillo, I. Egry, and B. Hallstedt, J. Mater. Sci. **47**, 8145 (2012).
[32] C. P. Royall and S. R. Williams, Phys. Reports **56**, 1 (2015).
[33] T. M. Truskett, S. Torquato, and P. G. Debenedetti, Phys. Rev. E **62**, 993 (2000).
[34] G. Kresse and J. Furthmüller, Comput. Mater. Sci. **6**, 15 (1996).
[35] D. M. Ceperley and B. J. Alder, Phys. Rev. Lett. **45**, 566 (1980); J. P. Perdew and A. Zunger, Phys. Rev. B **23**, 5048 (1981).
[36] N. Jakse and A. Pasturel, Sci. Rep. (Nature) **3**, 3135 (2013).
[37] J. Brillo, I. Egry, and J. Westphal, Int. J. Mater. Res. **99**, 2 (2008).
[38] W. E. Alley and B. J. Alder, Phys. Rev. A **27**, 3158 (1983); B. J. Palmer, Phys. Rev. E **49**, 359 (1994).
[39] N. Jakse, J. F. Wax, and A. Pasturel, J. Chem. Phys. **126**, 234508 (2007).
[40] M. P. Allen and D. J. Tidesley, *Computer Simulations of Liquids*. (Oxford University Press, Oxford, 1989).
[41] J. D. Honeycutt and H. C. Andersen, J. Phys. Chem. **91**, 4950 (1987).
[42] A. Pasturel and N. Jakse, J. Non-Cryst. Solids **42**, 176 (2015).
[43] A. Pasturel and N. Jakse, J. Phys. Cond. Matter **27**, 325104 (2015).
[44] N. Jakse and A. Pasturel, Mod. Phys. Lett. B **20**, 655 (2006).
[45] S. Y. Wang, M. J. Kramer, M. Xu, S. Wu, S. G. Hao, D. J. Sordelet, K. M. Ho, and C. Z. Wang, Phys. Rev. B **79**, 144205 (2009).
[46] H. Lou, X. Wang, Q. Cao, D. Zhang, J. Zhan, T. Hu, H.-k. Mao, and J.-Z. Jiang, PNAS **110**, 10068 (2013).
[47] J. Brillo, A. Bytchkov, I. Egry, L. Hennet, G. Mathiak, I. Pozdnyakova, D. L. Price, D. Thiaudiere, and D. Zanghi, J. Non-Cryst. Solids **352**, 4008 (2006).
[48] O. S. Roik, O. V. Samsonnikov, V. P. Kazimirov, V. E. Sokolskii, and S. M. Galushko, J. Mol. Liquids **151**, 42 (2010).
[49] A. Pasturel, E. S. Tasci, M. H. F. Sluiter, and N. Jakse, Phys. Rev. B **81**, 140202(R) (2010).
[50] W. Y. Wang, J. J. Han, H. Z. Fang, J. Wang, Y. F. Liang, S. L. Shang, Y. Wang, X. J. Liu, L. J. Kecskes, S. N. Mathaudhu, X. Hui, and Z. K. Liu, Acta Mater. **97**, 75 (2015).
[51] L. H. Xiong, H. Yoo, H. B. Lou, X. D. Wang, Q. P. Cao, D. X. Zhang, J. Z. Jiang, H. L. Xie, T. Q. Xiao, S. Jeon, and G. W. Lee, J. Phys. Condens. Matter **27**, 035102 (2015).
[52] H. Tanaka, Faraday Discuss. **167**, 9 (2003).
[53] T. Iwashita, D. M. Nicholson, and T. Egami, Phys. Rev. Lett. **110**, 205504 (2013).
[54] N. Jakse, A. Nassour, and A. Pasturel, Phys. Rev. B **85**, 174201 (2012).
[55] N. Jakse and A. Pasturel, Appl. Phys. Lett. **105**, 131905 (2014).
[56] Y. Rosenfeld, Phys. Rev. A **15**, 2545 (1977); J. Phys.: Condens. Matter **11**, 5415 (1999).
[57] M. Dzugutov, Nature **381**, 137 (1996).
[58] A. Samantha, S. M. Ali, and S. K. Ghosh, Phys. Rev. Lett. **87**, 245901 (2001); J. Chem. Phys. **123**, 084505 (2005).
[59] J. J. Hoyt, M. Asta, and B. Sadigh, Phys. Rev. Lett. **85**, 594 (2000).
[60] G. X. Li, C. S. Liu, and Z. G. Zhu, Phys. Rev. B **71**, 094209 (2005).
[61] J. Mittal, J. R. Errington, and T. Truskett, J. Phys. Chem. B **111**, 10054 (2007).
[62] J. Mittal, J. R. Errington, and T. M. Truskett, Phys. Rev. Lett. **96**, 177804 (2006).
[63] B. S. Jabes and C. Chakraverty, J. Chem. Phys. **136**, 144507 (2012).
[64] M. Argawal, M. Singh, B. S. Jabes, and C. Chakraverty, J. Chem. Phys. **134**, 014502 (2011).
[65] M. Singh, M. Argawal, D. Dhabal, and C. Chakraverty, J. Chem. Phys. **137**, 024508 (2012).
[66] K. Binder and W. Kob, *Glassy Materials and Disordered Solids* (World Scientific Publishing, Singapore, 2005).
[67] F. Demmel, D. Szubrin, W. C. Pilgrim, and C. Morkel, Phys. Rev. B **84**, 014307 (2011).
[68] F. Kargl, H. Weis, T. Unruh, and A. Meyer, J. Phys.: Conf. Ser. **340**, 012077 (2012).
[69] A. Meyer, Phys. Rev. B **81**, 012102 (2010).